Contents lists available at SciOpen

Food Science and Human Wellness

journal homepage: https://www.sciopen.com/journal/2097-0765

Bakuchiol ameliorates glycolipid homeostasis by reducing inflammation

Zhenhua Liu[a,b,c,1], Xiaoqing Xu[a,1], Zhenhua Liang[a,1], Yixiao Chen[a,b], Qiuyi Wang[a,b], Wenyi Kang[a,b,c,d,*], Yan Zhang[a,e,f,*], Bin Cong[e,*]

[a] National R&D Center for Edible Fungus Processing Technology, Henan University, Kaifeng 475004, China
[b] Joint International Research Laboratory of Food & Medicine Resource Function, Kaifeng 475004, China
[c] College of Agriculture, Henan University, Kaifeng 475004, China
[d] Shenzhen Research Institute of Henan University, Shenzhen 518000, China
[e] Hebei Key Laboratory of Forensic Medicine, College of Forensic Medicine, Hebei Medical University, Shijiazhuang 050017, China
[f] Hebei Food Safety Key Laboratory, Hebei Food Inspection and Research Institute, Shijiazhuang 050091, China

ARTICLE INFO

Article history:
Received 7 November 2023
Received in revised form 18 January 2024
Accepted 7 February 2024

Keywords:
Bakuchiol
Diabetes
Insulin resistance
Proteomic
Inflammation

ABSTRACT

Inflammatory stimulation plays a significant role in the development and worsening of insulin-resistant diabetes. Therefore, it is crucial to identify therapeutic agents that can alleviate insulin resistance by targeting inflammation. Here, we present evidence that Bakuchiol (BL), a monoterpene phenolic compound first discovered from *Psoralea corylifolia* L. as traditional Chinese medicine, can effectively improve insulin resistance in diabetic mice through anti-inflammation. Our findings demonstrate that BL alleviates inflammation by inhibiting the toll-like receptor 4/nuclear factor κB/mitogen-activated protein kinase axis, consequently enhancing insulin receptor signaling through the c-Jun N-terminal kinase/suppressors of cytokine signaling 3/insulin receptor substrate1 pathway and improving glucolipid homeostasis. Furthermore, the insulin recovery achieved with BL (60 mg/kg) was comparable to that of metformin (200 mg/kg). These results provide further support for considering BL as a potential treatment option for insulin-resistant diabetes mellitus.

1. Introduction

Diabetes mellitus (DM) is currently the leading cause of death, cardiovascular complications, and health care burden worldwide. It affects more than 500 million people, with the vast majority of cases being type 2 diabetes mellitus (T2DM)[1-3]. T2DM is a systemic metabolic disease characterized by persistent hyperglycemia and insulin resistance (IR). IR refers to a pathophysiological state in which the organs or cells targeted by insulin have reduced sensitivity to its effects. This leads to reduced glucose uptake and utilization mediated by insulin[4-6].

The development of IR is often accompanied by chronic inflammation. Inflammatory factors can interfere with the insulin signaling pathway and exacerbate IR[7]. Inflammation leading to IR is mainly dependent on the insulin receptor substrate 1 (IRS1) in the IRS1/phosphatidylinositol-3-hydroxy kinase (PI3K)/protein kinase B (Akt) signaling pathway. Inflammatory secretion can activate the mitogen-activated protein kinase (MAPK) signaling pathway, prompting c-Jun N-terminal kinase (JNK) to activate the serine and threonine residues (Ser/Thr) of IRS1, inhibiting the phosphorylation of the normal tyrosine (Tyr) site of IRS1, which in turn inhibits the PI3K/Akt signaling pathway and attenuates glucose transporter 4 (GLUT4) translocation in adipose cells, which results in reduced insulin utilization in peripheral tissues and ultimately leads to IR[8]. Thus, IRS1 phosphorylation plays a key role in inflammation-induced impaired insulin signaling and IR.

Natural products, particularly terpenoids such as gentiopicroside, resveratrol, hydroxytyrosol, andrographolide, and salvianolic

[1] These authors made equal contributions to this work.
[*] Correspondence authors.
E-mail address: hbydcongbin@126.com (B. Cong); snowwinglv@126.com (Y. Zhang); kangweny@hotmail.com (W.Y. Kang)
Peer review under responsibility of Tsinghua University Press.

Publishing services by Tsinghua University Press

http://doi.org/10.26599/FSHW.2023.9250052

acid, have been reported to have hypoglycemic effects and play an important role in the treatment of T2DM and its complications due to their effective action, mild process, and low toxic side effects[9-14]. Bakuchiol, the main active compound of the Chinese herbal medicine psoralen, has various pharmacological activities, including anti-inflammatory[15], tumor suppression[16], anti-influenza virus[17], antifungal effects[18]. It has also gained popularity as an ingredient in cosmetic skin care products due to its excellent antioxidant and anti-aging properties[19].

Psoralea corylifolia L. is a widely used herbal medicine with multiple pharmacological activities[20-21]. Bakuchiol (BL), isolated from *P. corylifolia* L., has been found to improve blood glucose levels in diabetic mice and attenuate hyperglycemia-induced diabetic cardiomyopathy[22-23]. However, underlying the ability of BL to improve disorders of glucolipid metabolism and IR induced by a high-fat diet (HFD) are still unknown. To shed light on this, we conducted a study utilizing proteomic and gut microbiome sequencing technologies with two cell lines: adipocytes and macrophages. The aim was to validate the regulatory mechanisms involved. Our findings indicate that BL inhibits Toll-like receptor 4 (TLR4)/nuclear factor κB (NF-κB) and MAPK signaling pathways, thereby activating suppressors of cytokine signaling 3 (SOCS3)/IRS1-mediated inhibition of insulin signaling. This study is the first to reveal the mechanisms through which the monoterpene BL effectively ameliorates inflammation-induced IR and glucolipid metabolism disorders caused by inflammation.

2. Materials and methods

2.1 Materials

Bakuchiol, 3-isobutyl-1-methylxanthine (IBMX), and dexamethasone (Dex) were purchased from Cayman (Ann Arbor, Michigan, USA) and detailed chemical information is listed in Table S1. Antibodies are listed in Table S2.

2.2 Mice and treatments

Male Kunming (KM) mice ((18 ± 2) g, 4–6 weeks old) were purchased from the Henan Provincial Laboratory Animal Center under license number SCXK 2017-0001. All animals were housed in a SPF environment with alternating cycles of constant temperature (25 ± 2) °C and constant humidity (40%–45%) with 12 h of light and 12 h of darkness. All experimental operations followed the Chinese Animal Welfare Law and were approved by the Ethics Committee of Henan University.

The diabetic mouse model was replicated as previously reported[24]. Briefly, animals were randomly assigned to each group (n = 10) and fed normal chow or HFD for 4 weeks. After this, high-fat mice were given a single intraperitoneal dose of 100 mg/kg of streptozocin (STZ). After successful modeling (fasting blood glucose (FBG) ≥ 16.7 mmol/L), BL was administered by gavage administration of 60, 30, and 15 mg/kg of BL (0.1 mL/10 g)[23]. The positive group was given metformin (200 mg/kg) by gavage. On day 30 of drug administration, mice were euthanized by eye removal, and serum was collected to determine glucose, lipid, oxidative stress and inflammation levels using assay kits (Jian Cheng Biotechnology Co., Ltd., Nanjing, China). The liver and pancreas were fixed in 4% (*V/V*) paraformaldehyde and embedded in paraffin, sections were stained with hematoxylin and eosin (H&E) to assess morphology. The epididymal fat and cecum contents were rapidly frozen using liquid nitrogen for later analysis.

2.3 Proteomic analysis of epididymal fat in mice

Quantitative protein isobaric tagging (IBT) analysis was performed as described previously[25]. Nine mice were randomly selected from the control group, model group and BL (60 mg/kg) group, respectively, and the epididymal adipose tissues of every 3 mice were combined into 1 sample, resulting in a total of 9 samples for the proteomic experimental study. Detailed methods are described in the supporting information.

2.4 16S rRNA sequencing and determination of short-chain fatty acids (SCFAs)

DNA extraction from cecum contents was performed as previously described[26]. DNA concentration was measured using the Equalbit dsDNA HS Assay Kit, amplified by polymerase chain reaction (PCR) and library construction, and sequenced using Illumina MiSeq/Novaseq (Illumina, San Diego, CA, USA). The concentration of SCFAs in the cecum contents was analyzed by high performance liquid chromatography (HPLC), following a modified protocol previously described to determine[24].

2.5 Cell culture

The 3T3-L1 adipocytes and RAW264.7 cells were purchased from the cell bank of the Chinese Academy of Sciences (Shanghai, China). The cells were maintained in DMEM medium (with a mixture of 10% neonatal bovine serum and 1% penicillin) and placed in an incubator at 37 °C and 5% CO_2. The cells could be passaged when the cell fusion was about 80%. For adipocyte differentiation, cells that had been exposed to inhibition were induced with medium A (containing 0.5 mmol/L IBMX, 1 μmol/L Dex and 10 μg/mL insulin) on day 4 after cell inoculation and maintained with medium B (containing 10 μg/mL insulin) for 2 days on day 7, after which they were replaced with normal medium for 2 days. For the RAW264.7 cell inflammation model, the cells were inoculated and incubated for 24 h. After this, they were pretreated with BL for 1 h. At the same time as the model group, the cells were treated with 1 μg/mL LPS for 24 h.

2.6 Cell viability

After treating of 3T3-L1 preadipose or RAW 264.7 cells with different concentrations of BL (120, 60, 30, 15 and 7.5 μmol/L) for 24 h, the cells were then incubated for 4 h with MTT solution (10 μL) protected from light. Next, the medium was discarded and DMSO (100 μL) was added to dissolve the blue-purple crystals. The cells were further incubated at 37 °C for 10 min, and the absorbance was measured at 490 nm using an enzyme marker.

2.7 Cellular Oil Red O staining

The differentiated adipocytes were washed three times with phosphate buffered saline (PBS) after discarding the medium, and the cells were fixed with 10% paraformaldehyde for 40 min. The cells were then rinsed three times with PBS buffer slowly, and the cells were stained with Oil Red O staining solution (0.25 g of Oil Red O powder dissolved in 100 mL of isopropanol) for 30 min. The staining solution was discarded, the cells were rinsed 3 times with PBS and photographed with an inverted microscope.

2.8 Western blot analysis

Cells or epithelial fat was lysed using RIPA lysis buffer on ice for 30 min. Then, lysates were centrifuged at 12 000 r/min for 10 min at 4 °C and subjected to sodium dodecyl sulfate-polyacrylamide gel electrophoresis. Western blot was performed as described previously[27]. Immunoblotting was performed using specific antibodies to assess the expression of different proteins.

2.9 Quantitative real time-polymerase chain reaction (qPCR)

Total RNA from cells was extracted with TRIzol, and gDNA was removed by a kit (TaKaRa) and reverse transcribed to cDNA. qPCR analysis was performed using TB Green® Premix Ex *Taq*™ II (Tli RNaseH Plus) in a gradient PCR detection system (MyCycler™Thermal Cycler). mRNA expression was normalized to *GAPDH*. The primer sequences are listed in the Table S3.

2.10 Immunofluorescence

RAW264.7 cells were washed 3 times slowly with PBS (3 min each time) and fixed with 4% paraformaldehyde for 30 min, followed by permeabilization with 0.5% TritonX-100 for another 15 min. Cells were blocked with 10% goat serum for 1 h at room temperature and then incubated overnight at 4 °C with the primary antibody (NF-κB p65). After washing with PBS, the cells were incubated with Alexa Fluor-coupled secondary antibody for 2 h at room temperature and protected from light. Afterward, the nuclei were stained with 4′,6-diamidino-2-phenylindole (DAPI) solution for 5 min in the dark and images were captured using a laser confocal fluorescence microscope (Nikon-A1R/STORM).

2.11 Flow cytometry

RAW264.7 cells were collected in EP tubes, washed with DMEM, and processed according to the reactive oxygen species (ROS) kit instructions[28]. After passing through a 300-mesh nylon sieve, the cells were tested on the instrument. Flow cytometry analysis was performed using a FACSArial III flow cytometer (BD FACSVerse, USA). The data were analyzed using FlowJo software (V.10.4, FlowJo, USA).

2.12 Statistical analysis

All experimental data are expressed as the mean ± standard deviation (SD) and were analyzed by SPSS 25.0 (SPSS Inc.). Unpaired Student's *t*-test was used to compare between 2 groups and multiple comparisons were assessed by one-way ANOVA with Turkey' tests. Statistical significance defined as $P < 0.05$.

3. Results

3.1 BL lowers the levels of glycolipids and inflammatory factors in T2DM mice

To determine the hypoglycemic function of an isoprenoid phenolic heteroterpenoid (BL structural formula as shown in Fig. 1A), the effects of BL on glycemic parameters and insulin levels in diabetic mice were first evaluated. The level of FBG, glycated serum protein (GSP) in mice were significantly reduced by BL (Figs. 1B and C), and the effect of BL was superior to that of metformin. Meanwhile, the level of insulin was found to be significantly increased (Fig. 1D). To shed light on the mechanism of blood glucose lowering by BL, IBT quantitative proteomic analysis was performed by mass spectrometry. In total, 4 940 proteins were quantified in mice epididymal fat from control, model and BL treatment groups; 331 of these proteins were significantly differentially expressed in the treatment group compared to the model group (fold change > 1.5, $P < 0.05$); 177 were upregulated and 154 were downregulated in expression, and 6 proteins were randomly selected from each of these groups for expression validation (Figs. S1A and B).

Enrichment and integration analysis of biological processes of differentially expressed proteins according to Gene Ontology (GO), ranked by the size of the enrichment factor, revealed that BL treatment resulted in the most significant anti-inflammatory function (negative regulation of cytokine secretion in immune). In addition, intestinal regulation (pancreatic fluid secretion, intestinal cholesterol absorption), lipid metabolism (triglycerides, plasma lipoproteins and cholesterol)[29] and antioxidant (oxidoreductase activity and retinoid metabolism) functions were also altered (Fig. 1E). To further confirm the proteomic results, a stepwise validation of the biological processes mentioned above was carried out. The first was the validation of the negative regulation of cytokine secretion. The levels of interleukin 6 (IL-6), tumor necrosis factor α (TNF-α), (Fig. 1F), and IL-1β (Fig. S1C) in mouse serum were measured by enzyme-linked immunosorbnent assay (ELISA), and BL was found to significantly reduce the STZ-induced elevation of inflammatory factors.

This was followed by the validation of the regulatory function of the gut, as multiple studies have previously shown that intestinal microbiota may regulate obesity and metabolic syndrome[30-32]. To this end, 16S rRNA sequencing was conducted on each group of cecum content samples. The results revealed that BL not only enhanced the diversity of the colony (Fig. S1D), but also reduced the abundance of Lachnospiraceae and increased the abundance of *Roseburia* (Fig. S1E). Lachnospiraceae, a core bacterium of the intestine, provides energy to the host mainly through the production of acetic acid[33]; while *Roseburia*, an anti-inflammatory factor, can produce large amounts of butyric acid to interact with the host[34]. To further validate the 16S rRNA sequencing results, the abundance of SCFAs (acetic acid, propionic acid, and butyric acid) in the cecum contents was examined using HPLC. The results showed that the abundance of acetic acid significantly decreased, butyric acid significantly increased, and propionic acid did not change significantly after BL treatment (Fig. S1F).

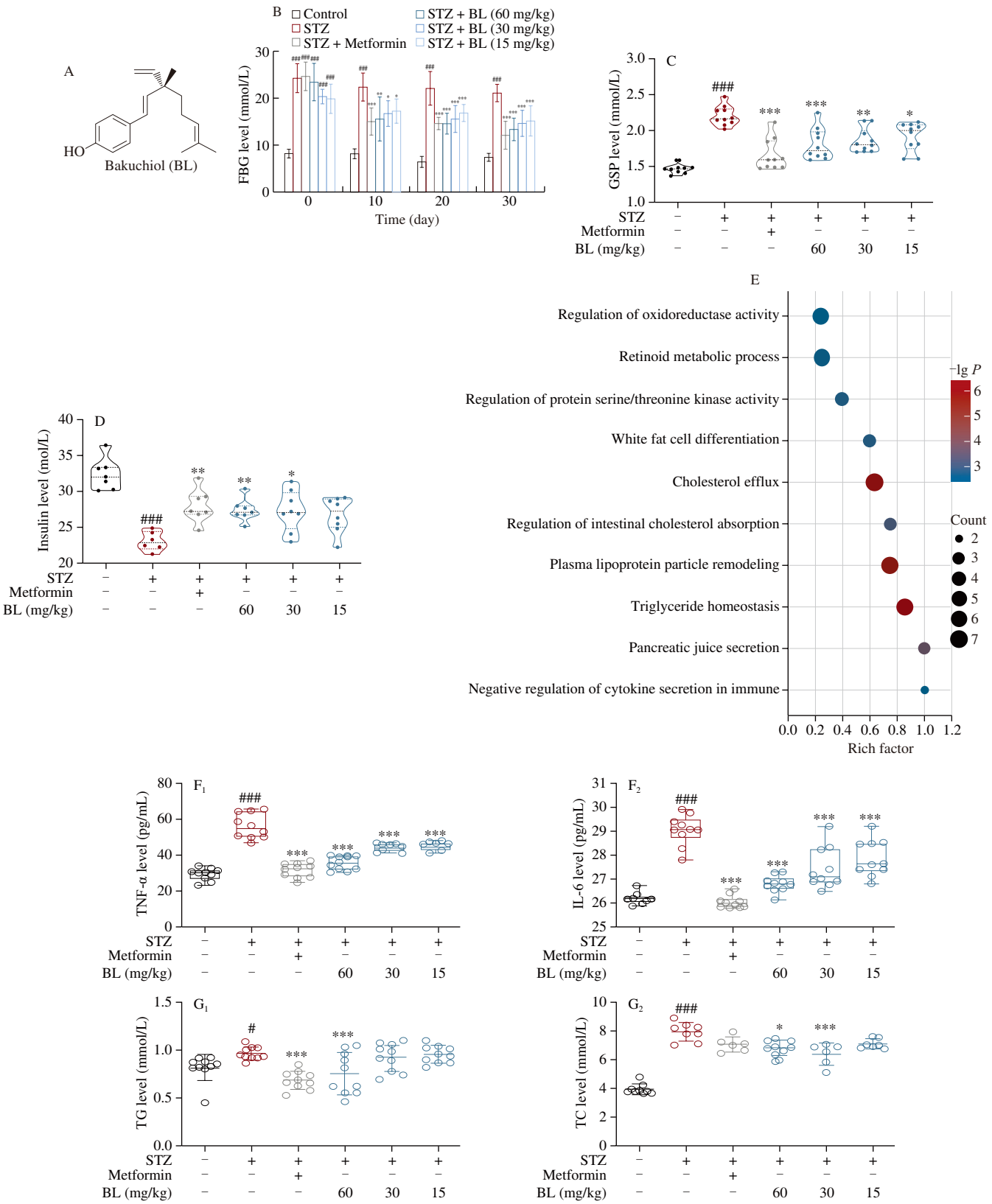

Fig. 1 The therapeutic effect of bakuchiol (BL) on high-fat, high-glucose combined with STZ in T2DM based on proteomic GO analysis. (A) Chemical structure of BL. (B) Effect of BL on FBG in mice. (C) Effect of BL on GSP in mice ($n = 10$). (D) Effect of BL on insulin levels in mouse serum ($n \geq 6$). (E) Top 10 GO entries obtained from the integration of significantly different protein enrichments in the BL treatment and model groups in proteomics. (F) Effects of BL on serum levels of inflammatory factors TNF-α and IL-6 in mice ($n = 10$). (G) Effect of BL on serum triglyceride (TG) and total cholesterol (TC) levels in mice ($n \geq 6$). (H) Effect of BL on serum high-density lipoprotein cholesterol (HDL-C) and low-density lipoprotein cholesterol (LDL-C) levels in mice ($n = 10$). (I) Pathological effects of BL on mouse pancreatic tissue. (J) Effect of BL on pathological effects on mouse liver tissues. (K) Effect of BL on malondialdehyde (MDA) and total antioxidant capacity (T-AOC) in mice ($n \geq 6$). Data expressed as mean ± SD. $^{###}P < 0.001$, $^{#}P < 0.05$ *vs.* control group; $^{***}P < 0.001$, $^{**}P < 0.01$, $^{*}P < 0.05$ *vs.* diabetes group.

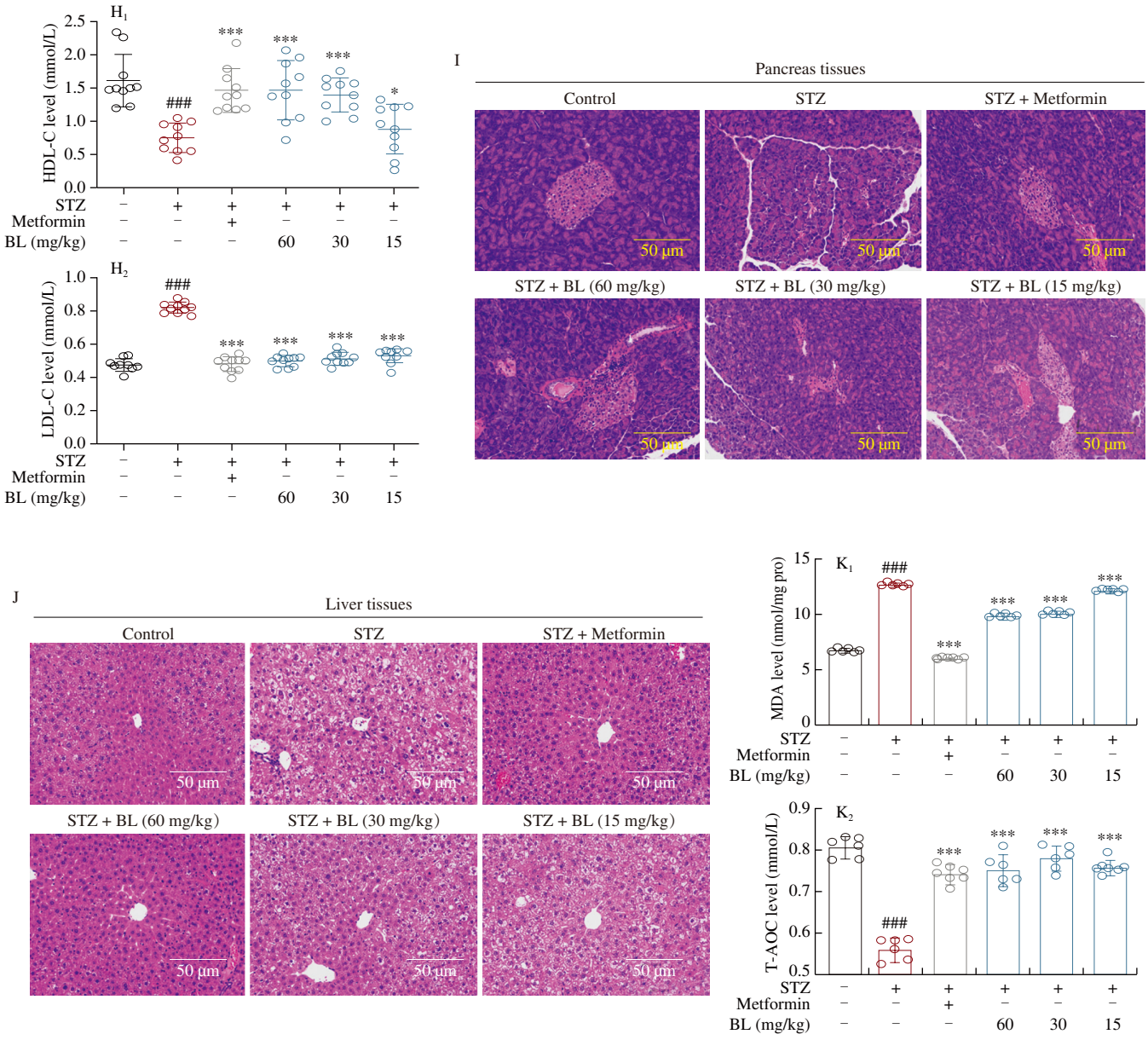

Fig. 1 (*Continued*)

This corresponded to the microbiota sequencing results and further demonstrated that BL can interact with the host through intestinal microorganisms and their metabolites to perform anti-inflammatory functions.

For the validation of lipid metabolism function, it has been shown that abnormal lipid metabolism may be due to the long-term elevated blood glucose level in mice and the conversion of large amounts of sugar to fat[34]. The results indicated that BL effectively reduced serum levels of triglyceride (TG) and total cholesterol (TC), and low-density lipoprotein cholesterol (LDL-C) (Figs. 1G and H). Additionally, it elevated high-density lipoprotein cholesterol (HDL-C) levels (Fig. 1H). Moreover, through H&E staining, it was observed that BL had an impact on the pancreas of diabetic mice, the alveolar cells were swollen and enlarged, irregularly arranged, with some degeneration and necrosis, and the inflammatory infiltration was obvious (Fig. 1I). In the liver, the cells were disorganized, locally deformed and necrotic, with a whitish field of view under the microscope, and the occurrence of steatosis, hepatocellular enlargement accompanied by inflammatory infiltration (Fig. 1J), while BL ameliorated the damage of liver and pancreatic tissues in diabetic mice. Furthermore, the results of significantly reduced malondialdehyde (MDA) level (Fig. 1K) and significantly increased catalase (CAT), superoxide dismutase (SOD) (Figs. S1G and H) and total antioxidant capacity (T-AOC) levels (Fig. 1K) also indicated that BL could effectively attenuate tissue peroxidative damage, which validated the predicted results of the proteomic function.

The above evidence suggests that including intestinal metabolites, the pathological basis of IR and oxidative stress-induced inflammation, all suggest that BL is likely to exert its hypoglycemic function mainly through anti-inflammation, and we will next investigate how BL regulates glucose homeostasis through anti-inflammation as well.

3.2 BL ameliorates IR in 3T3-L1 adipocytes

Blockage of insulin receptor signaling is the main mechanism of IR diabetes mellitus and is also often accompanied by inflammation[9]. Hence, to confirm the effect of BL on IR and hypoglycemic activity, we first studied the role of BL in 3T3-L1 adipocytes. The MTT assay revealed that BL was not cytotoxic at concentrations ranging from 3.25 to 50 μmol/L (Fig. 2A). After maturation of adipocyte-induced differentiation (Fig. S2), BL was found to significantly promote the glucose uptake capacity of adipocytes (Fig. 2B) and significantly promoted GLUT4 transcription (Fig. 2C) and protein expression levels (Fig. 2D), comparable to the effect of the positive control sodium pervanadate (Van). To elucidate the hypoglycemic pathway of BL in adipocytes, we found that BL activated the IRS1/PI3K/Akt axis, the central link of the insulin pathway, and that p110α, the catalytic subunit of PI3K, was significantly increased in expression and phosphorylation levels of IRS1 and Akt by BL (Figs. 2E and F). To further validate this result, the pathway-specific inhibitor Wortmannin (Wort) was used and the expression levels of p110α and Akt were examined (Figs. 2G and H). The results confirmed that BL could improve IR in 3T3-L1 adipocytes by activating the PI3K/AKT signaling pathway.

3.3 BL inhibited LPS-induced inflammation and oxidative stress in RAW264.7 cells

A model of LPS-induced inflammation in RAW264.7 cells was used to confirm the anti-inflammatory effect of BL. After finding no effect of BL on cell viability at concentrations ranging from 3.125 to 50 μmol/L by MTT assay (Fig. 3A), 12.5 to 50 μmol/L was selected for the study. BL significantly inhibited NO secretory capacity (Fig. 3B), inducible nitric oxide synthase (iNOS) transcript level (Fig. 3C), and protein expression (Fig. 3D), which are signature molecules of M1 macrophages induced by TLR ligands and inflammatory cytokines[35]. BL also significantly inhibited the transcription (Fig. 3E) and protein expression level (Fig. 3F) of cyclooxygenase 2 (COX-2), a common inducible enzyme in the inflammatory response. Moreover, BL likewise decreased the levels of pro-inflammatory cytokines such as IL-6 (Fig. 3G) and TNF-α (Fig. 3H),

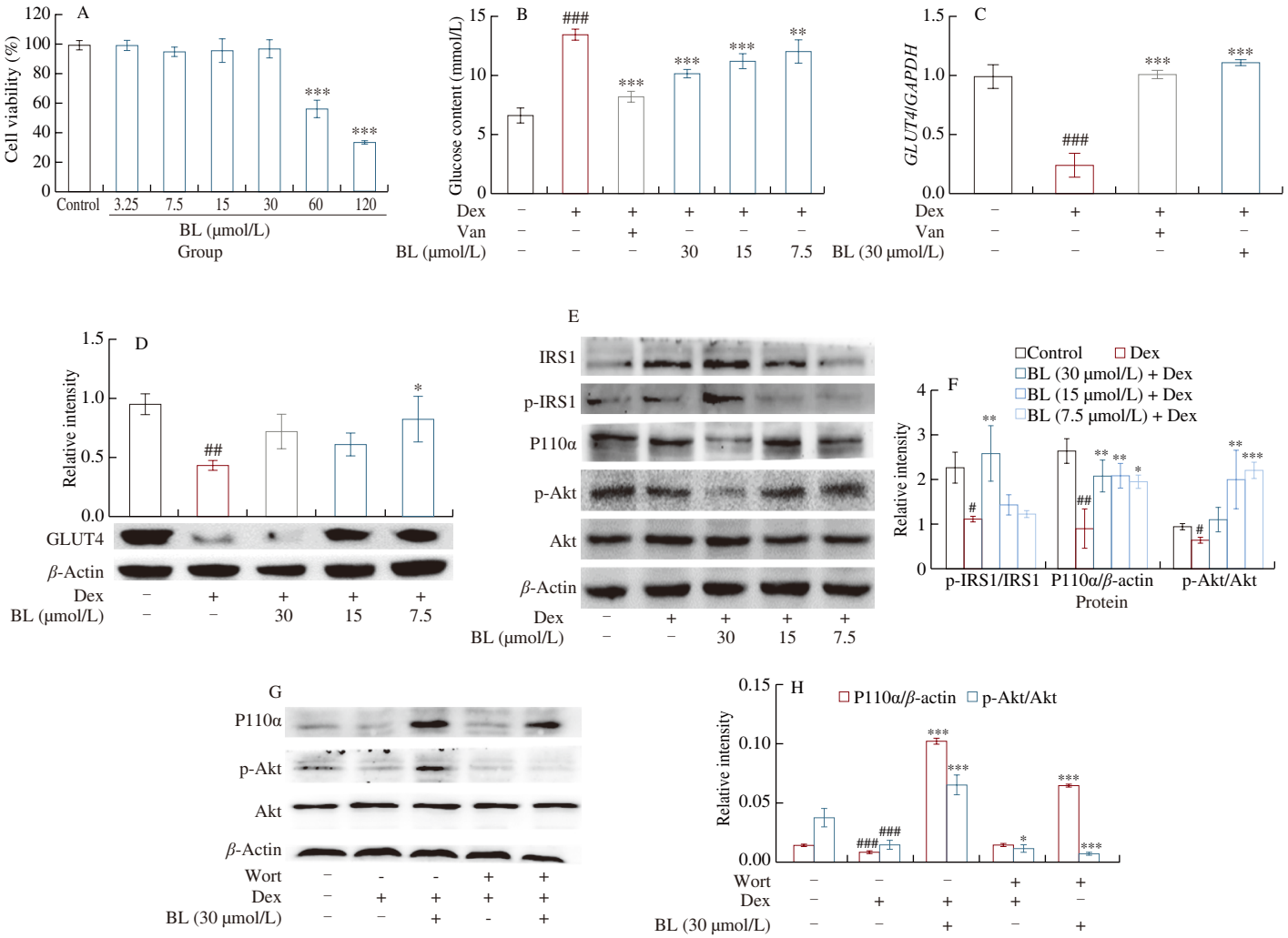

Fig. 2 BL ameliorates IR in 3T3-L1 adipocytes via IRS1/PI-3K/Akt signaling pathway. (A) Effect of BL on the viability of 3T3-L1 preadipocytes ($n = 3$). (B) Effect of BL on glucose content in the supernatant of 3T3-L1 adipocytes ($n = 3$). (C-D) qPCR and Western blot to detect the effect of BL on GLUT4 ($n = 3$). (E-F) Effect of BL on IRS1/PI3K/Akt-related protein expression ($n = 3$). (G-H) Effect of BL on the expression of PI3K/Akt signaling pathway-related proteins after the action of the pathway inhibitor Wortmannin (Wort) ($n = 3$). Data expressed as mean ± SD. $^{\#}P < 0.05$, $^{\#\#\#}P < 0.001$ *vs.* control group; $^{*}P < 0.05$, $^{**}P < 0.01$, $^{***}P < 0.001$ *vs.* model group.

and chemokines such as macrophage inflammatory protein 1 (MIP-1α) (Fig. S3A) and monocyte chemoattractant protein 1 (MCP-1), (Fig. S3B).

We next sought to elucidate the mechanism by which BL reduces LPS-induced inflammation. In the proteome sequencing results of diabetic mice, the GO analysis also showed an enrichment of functions related to the activation of the MAPK pathway. Furthermore, BL treatment significantly inhibited LPS-induced phosphorylation levels of p38, extracellular regulated protein kinase (ERK) and JNK proteins in RAW264.7 cells (Fig. 4A). In addition, elevated TNF-α levels suggest that NF-κB can cause activation of inflammatory genes through nuclear translocation of the p65 component of the complex, while TLR, a component of the innate immune system, recognize the molecular pattern of microbial components and the TLR4/NF-κB signaling pathway can lead to organismal inflammation[36]. Therefore, we investigated the anti-inflammatory properties of BL on the TLR4/NF-κB signaling pathway. The results demonstrated that BL effectively suppressed the transcriptional levels of *TLR4*, *MyD88*, *TICAM1* (Fig. 4B), as well as NF-κB phosphorylation and inhibitor of NF-κB (IκB) expression (Fig. 4C) in RAW264.7 cells. Moreover, BL significantly

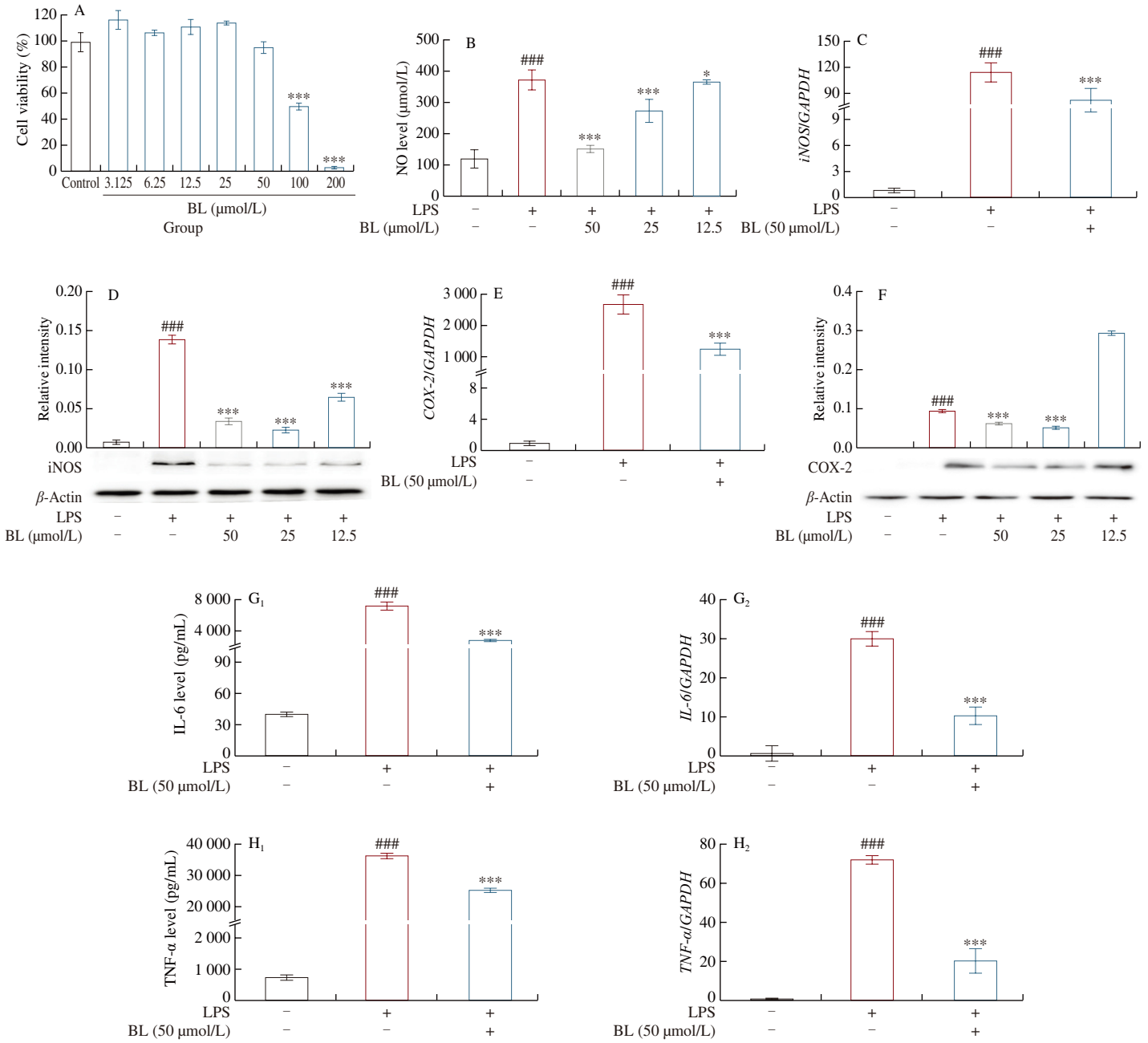

Fig. 3 Effect of BL on LPS-induced inflammation in RAW264.7 cells. (A) Effect of BL on the viability of RAW264.7 cells. (B) Effect of BL on NO secretion in RAW264.7 cells by nitrate reductase assay. (C) qPCR to detect the effect of BL on *iNOS* expression in RAW264.7 cells. (D) Western blot were used to assess the effect of BL on iNOS protein expression in RAW264.7 cells. (E) qPCR to detect the effect of BL on *COX-2* transcription in RAW264.7 cells. (F) The expression level of COX-2 protein in RAW264.7 cells was detected by Western blot. (G) Effect of BL on the secretion of IL-6 and its mRNA transcription in RAW264.7 cells. (H) Effect of BL on the secretion of TNF-α and its mRNA transcription in RAW264.7 cells. Data expressed as mean ± SD, $n = 3$. $^{###}P < 0.001$ *vs*. control group; $^{*}P < 0.05$, $^{***}P < 0.001$ *vs*. model group.

inhibited the nuclear translocation of NF-κB, as observed through laser confocal imaging (Fig. 4D). Additionally, flow cytometry analysis revealed that BL markedly reduced the ROS content induced by LPS in RAW264.7 cells (Fig. 4E). These experimental results suggest that BL inhibited LPS-induced inflammation and oxidative stress.

3.4 BL ameliorates IR in 3T3-L1 adipocytes via anti-inflammation

We aimed to elucidate the causal relationship between inflammation and IR in 3T3-L1 adipocytes. Transwell chambers were initially observed using an inverted microscope to study the migration process of RAW264.7 cells towards adipocytes (Fig. 5A). It was discovered that the treatment with BL hindered the infiltration of RAW264.7 cells into adipocytes (Fig. 5B). Likewise, BL reduced the elevation of inflammatory factors and chemokines induced by TNF-α stimulation in adipocytes (Figs. 5C, S4A and B). SOCS3, as a ubiquitinated linker protein, can competitively inhibit the phosphorylation of IRS1, leading to IR[37]. Thus, Western blot analysis revealed that BL significantly decreased the expression of SOCS3 and increased the phosphorylation level of IRS1. These findings indicate that BL effectively improves inflammation-induced IR in 3T3-L1 adipocytes (Fig. 5D). In addition, BL reduced NF-κB phosphorylation and IκB expression levels (Fig. 5E) that were elevated by TNF-α stimulation, and likewise decreased the phosphorylation levels of JNK (Fig. S4C), further confirming the promising anti-inflammatory and hypoglycemic effects of BL.

4. Discussion

T2DM remission is associated with the correction of obesity and islet β-cell dedifferentiation, and importantly, also with the correction of IR[38-39]. It is a type of metabolic disorder syndrome that is due to a genetic defect[40]. In this study, a high-fat and high-sugar diet combined with STZ was used to induce a T2DM mouse model with IR. STZ has a selective destructive effect on pancreatic β-cells, and the combination of high-fat and high-sugar diet feeding can prepare mice into a diabetes mellitus model that more closely resembles human suffering[41]. Metformin, as a clinical first-line drug, can be used by enhancing the affinity of insulin to its receptor[42]. While our results showed that BL possessed insulin recovery levels comparable to those of metformin, indicating the potential of BL to be developed as a hypoglycemic agent. To further understand the

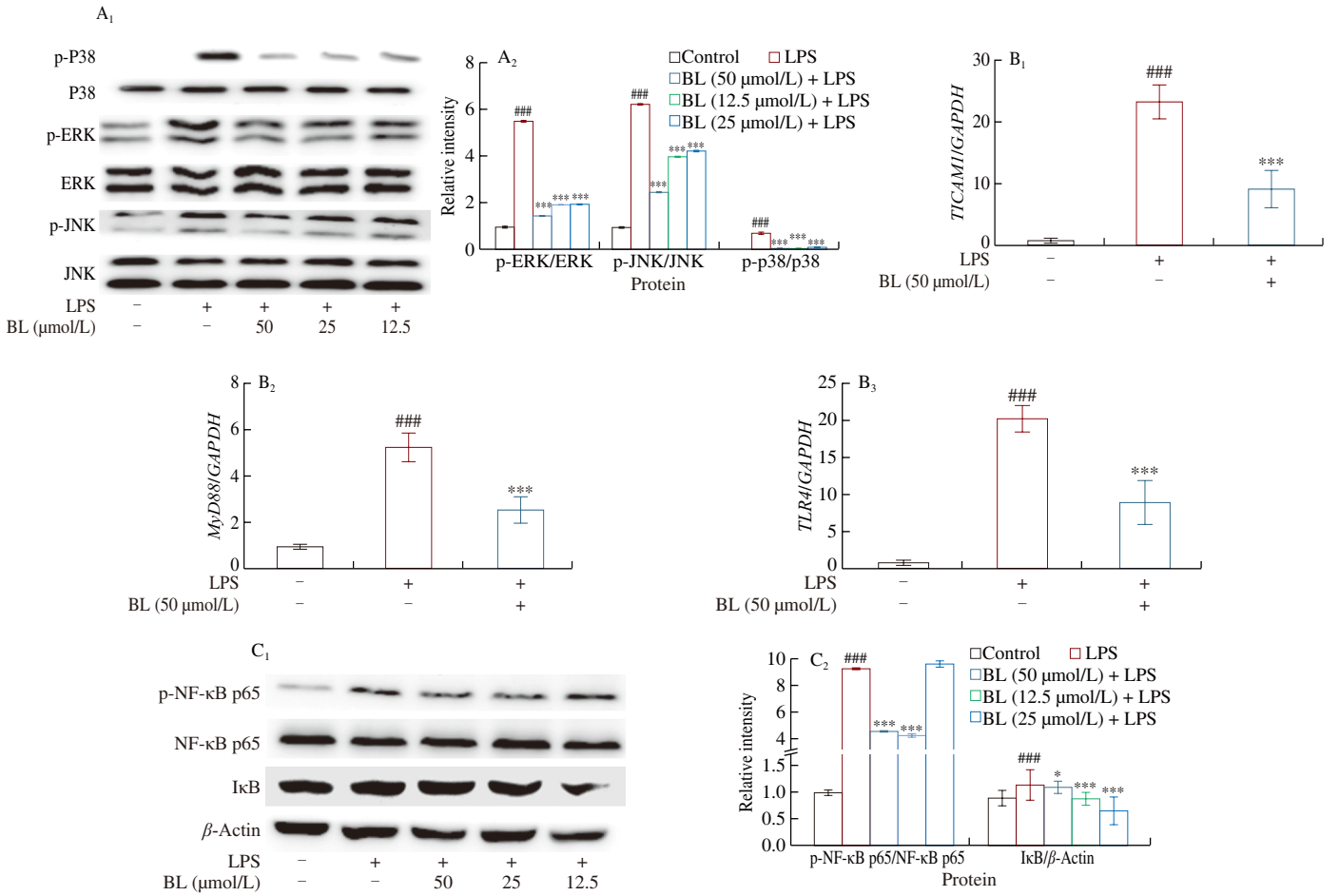

Fig. 4 BL inhibits inflammation in RAW264.7 cells via TLR4/NF-κB and MAPK signaling pathways. (A) The effect of BL on MAPK signaling pathway-related protein expression was analyzed by Western blot as well as quantified by Image J. (B) qPCR analysis of the expression levels of *TICAM1*, *MyD88* and *TLR4* in RAW264.7 cells. (C) The effect of BL on the expression of NF-κB signaling pathway-related proteins was analyzed by Western blot as well as quantified by Image J. (D) The effect of BL on p65 nuclear translocation was observed using laser confocal microscopy. (E) Flow cytometry detection of the effect of BL on LPS-induced ROS content in RAW264.7 cells and quantification by relative fluorescence intensity analysis. Data expressed as mean ± SD, $n = 3$. $^{###}P < 0.001$ *vs.* control group; $^{*}P < 0.05$, $^{***}P < 0.001$ *vs.* model group.

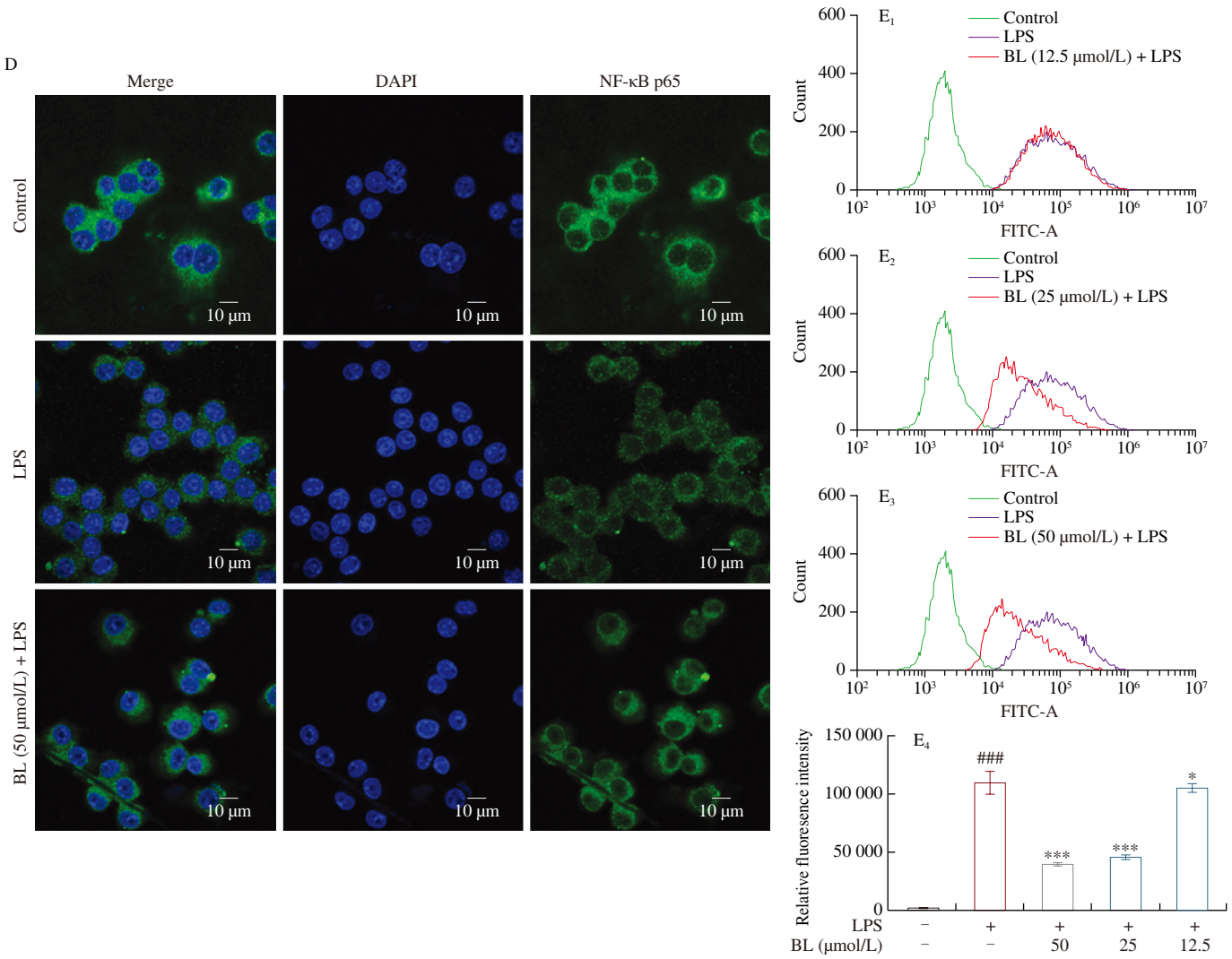

Fig. 4 (*Continued*)

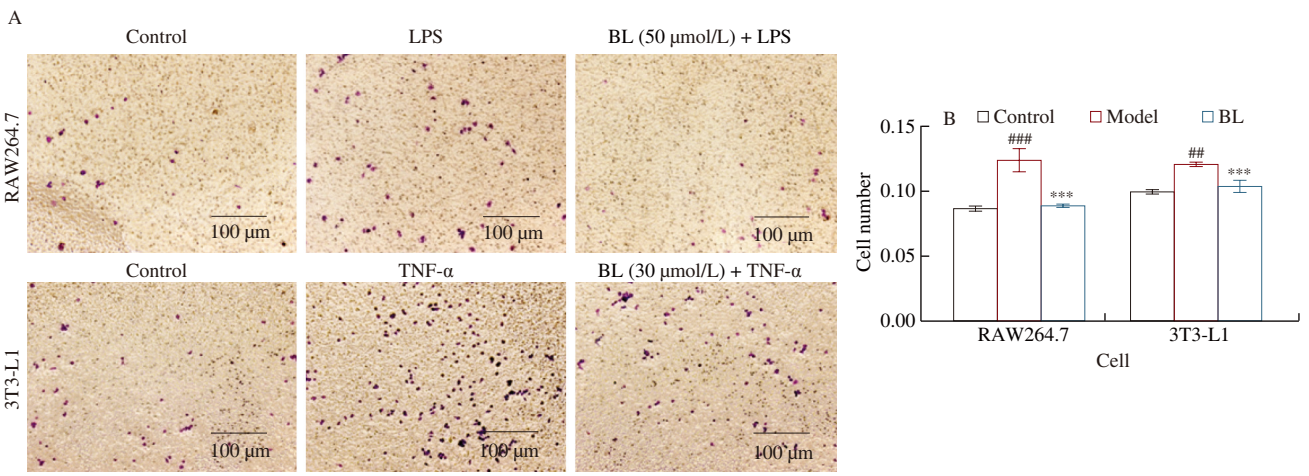

Fig. 5 BL modulates 3T3-L1 adipocytes IR through anti-inflammation. (A) Effect of BL on the migration of RAW264.7 cells to 3T3-L1 adipocytes. (B) The quantitative plot of relative migration rate analysis. (C) The mRNA expression of inflammation-related genes in 3T3-L1 adipocytes was quantified by qPCR analysis and normalized to *GAPDH*. (D) The effect of BL on the expression of SOCS3/IRS1 signaling pathway-related proteins in 3T3-L1 adipocytes was detected by Western blot as well as quantified by Image J. (E) The effect of BL on the expression of NF-κB signaling pathway-related proteins in 3T3-L1 adipocytes was analyzed by Western blot as well as quantified by Image J. Data expressed as mean ± SD, $n = 3$. $^{\#\#}P < 0.01$, $^{\#\#\#}P < 0.001$ *vs*. control group; $^{**}P < 0.01$, $^{***}P < 0.001$ *vs*. model group.

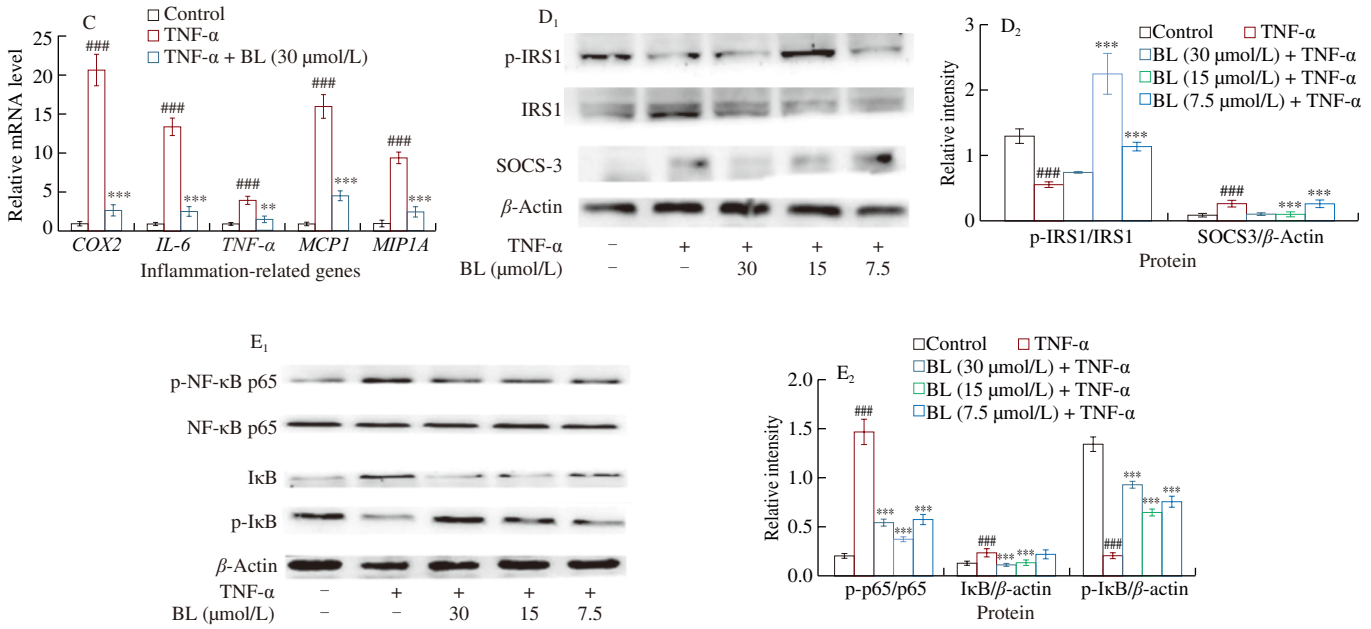

Fig. 5 (*Continued*)

underlying molecular mechanisms, we generated a proteomic profile of adipose tissue, and several enriched functions point to a strong correlation between the effects of BL and anti-inflammation. i) As a proven anti-inflammatory and antioxidant natural product, BL has been shown to modulate the abnormal production of inflammatory molecules and endogenous antioxidants[23,43-45]. And here we found antioxidant and retinoid processes that imply a protective effect of BL in inflammation and oxidative stress that accompany IR. ii) The regulation of gut microbes and their metabolites. Our results showed that BL significantly increased the abundance of *Roseburia* as well as butyrate, the main producer of butyrate, and several studies have shown its important role in T2DM[46-47]. Furthermore, it has been well established that the reduction of butyrate directly controls the inflammatory response of adipocytes, which further suggests to us that BL alleviates IR through anti-inflammatory factors[48-49]. iii) Importantly, the negative regulation of MAPK and cytokines points even more directly to the association of BL with anti-inflammation[50].

As the main target organ for T2DM, adipose tissue acts as an endocrine organ in the body, secreting a variety of adipokines that regulate systemic metabolism[51]. The differentiation of adipocytes is directly related to the occurrence of other metabolic diseases such as glucolipid metabolism. Therefore, we chose 3T3-L1 adipocytes, which are widely used in the study of glucolipid metabolism[52-53], as the subject of our *in vitro* study. The normal conduction of the insulin signaling pathway is required to ensure its biological effects. Any impairment in any of the links can lead to abnormal signaling and generate IR. Most of the new drugs under development and old drugs already approved for T2DM are focused on improving the PI3K/AKT axis transduction[54-55]. Dex is able to cause a decrease in insulin effect, leading to the development of diabetes mellitus[56]. We found that BL activated the IRS1/PI3K/Akt signaling pathway inhibited by Dex, demonstrating that BL increases insulin sensitivity in adipocytes *in vitro*.

Inflammatory stimuli are important factors in generating and exacerbating IR. Ameliorating IR by suppressing the inflammatory response is the focus of new drug development and clinical research. With this in mind, we induced the inflammatory state of RAW264.7 cells with LPS and found that BL confirmed its excellent anti-inflammatory activity by inhibiting the expression of TLR4/NF-κB/MAPK signaling pathway-related proteins. This is consistent with the results previously reported for BL[15,57]. IκB acts as a suppressor of NF-κB. After oxidative stress, IκB dissociates from NF-κB and NF-κB enters the nucleus to regulate the expression of related inflammatory factors[58]. The phosphorylation of IκB is mediated by IKK, which inhibits the binding of insulin receptors to IRS1, blocking the normal insulin transmission pathway and eventually leading to IR[59]. In addition, the MAPK signaling pathway of JNK activates the Ser307 site on IRS1, blocking the normal Tyr632 site phosphorylation, which in turn leads to IR[8,60]. The GO functional enrichment also indicates a potential link between MAPK and T2DM. Thus, the results of the present study suggest that BL exerts anti-inflammatory effects to improve IR by inhibiting the secretion of adipocyte chemokines through suppressing NF-κB, JNK, and SOCS3 protein expression. It also inhibits the recruitment of macrophages by adipocytes. Similar findings have been found in other terpenoids that ameliorate IR through anti-inflammation. For example, baicalin can improve IR by inhibiting the MAPK signaling pathway and cytoplasmic inflammation, activating the IRS1/PI3K/Akt axis and thus improving IR[61]. Additionally, lycopene[62] and geniposide[63] can also ameliorate IR through anti-inflammation.

5. Conclusion

The study investigated how BL helps reduce IR and improve glucolipid metabolism. It was discovered that BL reduces inflammation by inhibiting the TLR4/NF-κB and MAPK signaling pathways. As a result, BL improves IR by impacting the JNK/SOCS3/IRS1 pathway. This study offers valuable insights into the development of glucose-lowering medications involving BL.

Declaration of competing interest

Bin Cong is editor-in-chief, Yan Zhang and Wenyi Kang are associate editors for *Food Science and Human Wellness* and were not involved in the editorial review or the decision to publish this article. The authors declare that they have no known competing financial interests or personal relationships that could have appeared to influence the work reported in this paper.

Acknowledgments

This study was supported by National Key R&D Program of China (2022YFF1100300), and the Central Guidance on Local Science and Technology Development Found of Shenzhen, China (2021Szvup030).

Ethic approval and consent to participate

We declare that the ethical background to this study was approved by ethical committee (HUSOM2022-267).

Appendix A. Supplementary data

Supplementary data associated with this article can be found, in the online version, at http://doi.org/10.26599/FSHW.2023.9250052.

References

[1] M. Nazarzadeh, Z. Bidel, D. Canoy, et al., Blood pressure-lowering treatment for prevention of major cardiovascular diseases in people with and without type 2 diabetes: an individual participant-level data meta-analysis, Lancet Diabetes Endocrinol. 10(9) (2022) 645-654. https://doi.org/10.1016/s2213-8587(22)00172-3.

[2] X. Lin, Y. Xu, X. Pan, et al., Global, regional, and national burden and trend of diabetes in 195 countries and territories: an analysis from 1990 to 2025, Sci. Rep. 10(1) (2020) 14790. https://doi.org/10.1038/s41598-020-71908-9.

[3] W. Yang, J. Lu, J. Weng, et al., Prevalence of diabetes among men and women in China, New Engl. J. Med. 362(12) (2010) 1090-1101. https://doi.org/10.1056/nejmoa0908292.

[4] M. Roden, Mechanisms of disease: hepatic steatosis in type 2 diabetes-pathogenesis and clinical relevance, Nat. Clin. Pract. Endoc. 2(6) (2006) 335-348. https://doi.org/10.1038/ncpendmet0190.

[5] J. Steinberger, S.R. Daniels, Obesity, insulin resistance, diabetes, and cardiovascular risk in children, Circulation 107(10) (2003) 1448-1453. https://doi.org/10.1161/01.CIR.0000060923.07573.F2.

[6] F.S.A. Saadeldeen, Y. Niu, H. Wang, et al., Natural products: regulating glucose metabolism and improving insulin resistance, Food Sci. Hum. Wellness 9(3) (2020) 214-228. https://doi.org/10.1016/j.fshw.2020.04.005.

[7] A. Fuchs, D. Samovski, G.I. Smith, et al., Associations among adipose tissue immunology, inflammation, exosomes and insulin sensitivity in people with obesity and nonalcoholic fatty liver disease, Gastroenterology 161(3) (2021) 968-981. https://doi.org/10.1053/j.gastro.2021.05.008.

[8] H. Li, C. Wang, J. Zhao, et al., JNK downregulation improves olanzapine-induced insulin resistance by suppressing IRS1 Ser307 phosphorylation and reducing inflammation, Biomed. Pharmacother. 142 (2021) 112071. https://doi.org/10.1016/j.biopha.2021.112071.

[9] H. Xiao, X. Sun, Z. Lin, et al., Gentiopicroside targets PAQR3 to activate the PI3K/AKT signaling pathway and ameliorate disordered glucose and lipid metabolism, Acta Pharm. Sin. B 12(6) (2022) 2887-2904. https://doi.org/10.1016/j.apsb.2021.12.023.

[10] T. Cai, X. Ye, R. Li, et al., Resveratrol modulates the gut microbiota and inflammation to protect against diabetic nephropathy in mice, Front. Pharmacol. 11 (2020) 1-11. https://doi.org/10.3389/fphar.2020.01249.

[11] N. Wang, Y. Ma, Z. Liu, et al., Hydroxytyrosol prevents PM2.5-induced adiposity and insulin resistance by restraining oxidative stress related NF-κB pathway and modulation of gut microbiota in a murine model, Free Radical. Bio. Med. 141 (2019) 393-407. https://doi.org/10.1016/j.freeradbiomed.2019.07.002.

[12] H. Su, J. Mo, J. Ni, et al., Andrographolide exerts antihyperglycemic effect through strengthening intestinal barrier function and increasing microbial composition of *Akkermansia muciniphila*, Oxid. Med. Cell. Longev. 2020 (2020) 6538930. https://doi.org/10.1155/2020/6538930.

[13] L. Li, R. Li, R. Zhu, et al., Salvianolic acid B prevents body weight gain and regulates gut microbiota and LPS/TLR4 signaling pathway in high-fat diet-induced obese mice, Food Funct. 11(10) (2020) 8743-8756. https://doi.org/10.1039/d0fo01116a.

[14] M. Song, D. Tan, B. Li, et al., Gypenoside ameliorates insulin resistance and hyperglycemia via the AMPK-mediated signaling pathways in the liver of type 2 diabetes mellitus mice, Food Sci. Hum. Wellness 11(5) (2022) 1347-1354. https://doi.org/10.1016/j.fshw.2022.04.029.

[15] H. Lim, Y. Kim, B. Kim, et al., Bakuchiol suppresses inflammatory responses via the downregulation of the p38 MAPK/ERK signaling pathway, Int. J. Mol. Sci. 20 (2019) 3574. https://doi.org/10.3390/ijms20143574.

[16] L. Miao, X. Yun, R. Tao, et al., Bakuchiol exhibits anti-metastasis activity through NF-κB cross-talk signaling with AR and ERβ in androgen-independent prostate cancer cells PC-3, J. Pharmacol. Sci. 138 (2018) 1-8. https://doi.org/10.1016/j.jphs.2017.04.004.

[17] D. Zhang, S. Hamdoun, R. Chen, et al., Identification of natural compounds as SARS-CoV-2 entry inhibitors by molecular docking-based virtual screening with bio-layer interferometry, Pharmacol. Res. 172 (2021) 105820. https://doi.org/10.1016/j.phrs.2021.105820.

[18] H. Li, J. Liu, C. Liu, et al., Design, synthesis, and biological evaluation of membrane-active bakuchiol derivatives as effective broad-spectrum antibacterial agents, J. Med. Chem. 64(9) (2021) 5603-5619. https://doi.org/10.1021/acs.jmedchem.0c02059.

[19] H. Draelos, J. Gunt, S. Zeichner, et al., Clinical evaluation of a nature-based bakuchiol anti-aging moisturizer for sensitive skin, J. Drugs Dermatol. 19(12) (2020) 1181-1183. https://doi.org/10.36849/jdd.2020.5522.

[20] X. Wei, L. Lin, Q. Yuan, et al., Bavachin protects against diet-induced hepatic steatosis and obesity in mice, Acta Pharmacol. Sin. 44(7) (2023) 1416-1428. https://doi.org/10.1038/s41401-023-01056-z.

[21] M. Shi, Y. Zhang, M. Song, et al., Screening the marker components in *Psoralea corylifolia* L. with the aids of spectrum-effect relationship and component knock-out by UPLC-MS^2, Int. J. Mol. Sci. 19(11) (2018) 3439. https://doi.org/10.3390/ijms19113439.

[22] J.M. Krenisky, J. Luo, M.J. Reed, et al., Isolation and antihyperglycemic activity of bakuchiol from *Otholobium pubescens* (Fabaceae), a peruvian medicinal plant used for the treatment of diabetes, Biol. Pharm. Bull. 22(10) (1999) 1137-1140. https://doi.org/10.1248/bpb.22.1137.

[23] W. Ma, W. Guo, F. Shang, et al., Bakuchiol alleviates hyperglycemia-induced diabetic cardiomyopathy by reducing myocardial oxidative stress via activating the SIRT1/Nrf2 signaling pathway, Oxid. Med. Cell. Longev. 2020 (2020) 3732718. https://doi.org/10.1155/2020/3732718.

[24] J. Dong, Q. Liang, Y. Niu, et al., Effects of *Nigella sativa* seed polysaccharides on type 2 diabetic mice and gut microbiota, Int. J. Biol. Macromol. 159 (2020) 725-738. https://doi.org/10.1016/j.ijbiomac.2020.05.042.

[25] Q. Liang, J. Dong, S. Wang, et al., Immunomodulatory effects of *Nigella sativa* seed polysaccharides by gut microbial and proteomic technologies, Int. J. Biol. Macromol. 184 (2021) 483-496. https://doi.org/10.1016/j.ijbiomac.2021.06.118.

[26] X. Zhang, Z. Liang, G.I.N. Waterhouse, et al., Structural characteristics, anticoagulant and antithrombotic mechanism of a novel polysaccharide from *Rosa chinensis* Flos, Food Sci. Hum. Wellness 12(2) (2023) 407-415. https://doi.org/10.1016/j.fshw.2022.07.042.

[27] Y. Zhang, P. Lv, J. Ma, et al., Antrodia cinnamomea exerts an anti-hepatoma effect by targeting PI3K/AKT-mediated cell cycle progression *in vitro* and *in vivo*, Acta Pharm. Sin. B 12(2) (2022) 890-906. https://doi.org/10.1016/j.apsb.2021.07.010.

[28] Q. Tang, S. Chen, S.A.H. Rizvi, et al., Two alkaloids from *Delphinium brunonianum* Royle, their anti-inflammatory and anti-oxidative stress activity via NF-κB signaling pathway, Front. Nutr. 8 (2022) 1-11. https://doi.org/10.3389/fnut.2021.826957.

[29] L. Zhu, Z. She, X. Cheng, et al., Association of blood glucose control and outcomes in patients with COVID-19 and pre-existing type 2 diabetes, Cell Metab. 31(6) (2020) 1068-1077. https://doi.org/10.1016/j.cmet.2020.04.021.

[30] X. Yuan, R. Wang, B. Han, et al., Functional and metabolic alterations of gut microbiota in children with new-onset type 1 diabetes, Nat. Commun. 13(1) (2022) 6356. https://doi.org/10.1038/s41467-022-33656-4.

[31] Y. Kawano, M. Edwards, Y. Huang, et al., Microbiota imbalance induced by dietary sugar disrupts immune-mediated protection from metabolic syndrome, Cell 185(19) (2022) 3501-3519. https://doi.org/10.1016/j.cell.2022.08.005.

[32] B.J. Russell, S.D. Brown, N. Siguenza, et al., Intestinal transgene delivery with native *E. coli* chassis allows persistent physiological changes, Cell 185(17) (2022) 3263-3277. https://doi.org/10.1016/j.cell.2022.06.050.

[33] H. Guo, W. Chou, Y. Lai, et al., Multi-omics analyses of radiation survivors identify radioprotective microbes and metabolites, Science 370 (2020) 9097. https://doi.org/10.1126/science.aay9097.

[34] K. Machiels, M. Joossens, J. Sabino, et al., A decrease of the butyrate-producing species *Roseburia hominis* and *Faecalibacterium prausnitzii* defines dysbiosis in patients with ulcerative colitis, Gut 63(8) (2014) 1275-1283. https://doi.org/10.1136/gutjnl-2013-304833.

[35] S.A. Sonar, G. Lal, The iNOS activity during an immune response controls the CNS pathology in experimental autoimmune encephalomyelitis, Front. Immunol. 10 (2019) 1-13. https://doi.org/10.3389/fimmu.2019.00710.

[36] T. Wei, M. Chandy, M. Nishiga, et al., Cannabinoid receptor 1 antagonist genistein attenuates marijuana-induced vascular inflammation, Cell 185(10) (2022) 1676-1693. https://doi.org/10.1016/j.cell.2022.04.005.

[37] M.J.A. Haider, Z. Albaqsumi, F. Al-Mulla, et al., SOCS3 regulates dectin-2-induced inflammation in PBMCs of diabetic patients, Cells 11(17) (2022) 2670. https://doi.org/10.3390/cells11172670.

[38] P. Petrus, S. Lecoutre, L. Dollet, et al., Glutamine links obesity to inflammation in human white adipose tissue, Cell. Metab. 31(2) (2020) 375-390. https://doi.org/10.1016/j.cmet.2019.11.019.

[39] W. Ying, W. Fu, Y.S. Lee, et al., The role of macrophages in obesity-associated islet inflammation and β-cell abnormalities, Nat. Rev. Endocrinol. 16(2) (2020) 81-90. https://doi.org/10.1038/s41574-019-0286-3.

[40] C. Ning, Y. Jiao, J. Wang, et al., Recent advances in the managements of type 2 diabetes mellitus and natural hypoglycemic substances, Food Sci. Hum. Wellness 11(5) (2022) 1121-1133. https://doi.org/10.1016/j.fshw.2022.04.004.

[41] B.L. Furman, Streptozotocin-induced diabetic models in mice and rats, Curr. Protoc. 1(4) (2021) e78. https://doi.org/10.1002/cpz1.78.

[42] A.K. Madiraju, Y. Qiu, R.J. Perry, et al., Metformin inhibits gluconeogenesis via a redox-dependent mechanism *in vivo*, Nat. Med. 24(9) (2018) 1384-1394. https://doi.org/10.1038/s41591-018-0125-4.

[43] A. Bluemke, A.P. Ring, J. Immeyer, et al., Multidirectional activity of bakuchiol against cellular mechanisms of facial ageing: experimental evidence for a holistic treatment approach, Int. J. Cosmetic. Sci. 44(3) (2022) 377-393. https://doi.org/10.1111/ics.12784.

[44] H. Liu, W. Guo, H. Guo, et al., Bakuchiol attenuates oxidative stress and neuron damage by regulating Trx1/TXNIP and the phosphorylation of AMPK after subarachnoid hemorrhage in mice, Front. Pharmacol. 11 (2020) 712. https://doi.org/10.3389/fphar.2020.00712.

[45] A. Cariola, M. El Chami, J. Granatieri, et al., Anti-tyrosinase and antioxidant activity of meroterpene bakuchiol from *Psoralea corylifolia* (L.), Food Chem. 405 (2023) 134953. https://doi.org/10.1016/j.foodchem.2022.134953.

[46] F.H. Karlsson, V. Tremaroli, I. Nookaew, et al., Gut metagenome in European women with normal, impaired and diabetic glucose control, Nature 498(7452) (2013) 99-103. https://doi.org/10.1038/nature12198.

[47] M. Ren, H. Zhang, J. Qi, et al., An almond-based low carbohydrate diet improves depression and glycometabolism in patients with type 2 diabetes through Modulating gut microbiota and GLP-1: a randomized controlled trial, Nutrients 12(10) (2020). 3036. https://doi.org/10.3390/nu12103036.

[48] M. Knip, H. Siljander, The role of the intestinal microbiota in type 1 diabetes mellitus, Nat. Rev. Endocrinol. 12(3) (2016) 154-167. https://doi.org/10.1038/nrendo.2015.218.

[49] Z. Gao, J. Yin, J. Zhang, et al., Butyrate improves insulin sensitivity and increases energy expenditure in mice, Diabetes 58(7) (2009) 1509-1517. https://doi.org/10.2337/db08-1637.

[50] Y. Meng, P. Gharibani, A. Maisiyiti, et al., Su1886-sacral nerve stimulation inhibits the MAPK/NF-κb signaling pathway and promotes Treg-Th1/17 cell balance in TNBS-induced inflammation in rats, Gastroenterology 156(6) (2019) S-649. http://doi.org/10.1016/S0016-5085(19)38523-3.

[51] C.M. Kusminski, P.E. Bickel, P.E. Scherer, Targeting adipose tissue in the treatment of obesity-associated diabetes, Nat. Rev. Drug Discov. 15(9) (2016) 639-660. https://doi.org/10.1038/nrd.2016.75.

[52] J. Sun, P. Leng, X. Li, et al., Salvianolic acid A promotes mitochondrial biogenesis and mitochondrial function in 3T3-L1 adipocytes through regulation of the AMPK-PGC1α signalling pathway, Adipocyte 11(1) (2022) 562-571. https://doi.org/10.1080/21623945.2022.2116790.

[53] Z. Xu, D. Liu, D. Liu, et al., Equisetin is an anti-obesity candidate through targeting 11β-HSD1, Acta Pharm. Sin. B 12(5) (2022) 2358-2373. https://doi.org/10.1016/j.apsb.2022.01.006.

[54] T.Y. Liu, C.X. Shi, R. Gao, et al., Irisin inhibits hepatic gluconeogenesis and increases glycogen synthesis via the PI3K/Akt pathway in type 2 diabetic mice and hepatocytes, Clin. Sci. 129(10) (2015) 839-850. https://doi.org/10.1042/cs20150009.

[55] L. Plum, E. Rother, H. Münzberg, et al., Enhanced leptin-stimulated PI3k activation in the CNS promotes white adipose tissue transdifferentiation, Cell Metab. 6(6) (2007) 431-445. https://doi.org/10.1016/j.cmet.2007.10.012.

[56] S. Liu, L. Ma, X. Ren, et al., A new mouse model of type 2 diabetes mellitus established through combination of high-fat diet, streptozotocin and glucocorticoid, Life Sci. 286 (2021) 120062. https://doi.org/10.1016/j.lfs.2021.120062.

[57] A. Kumar, G. Sawhney, R. Kumar Nagar, et al., Evaluation of the immunomodulatory and anti-inflammatory activity of Bakuchiol using RAW264.7 macrophage cell lines and in animal models stimulated by lipopolysaccharide (LPS), Int. Immunopharmacol. 91 (2021) 107264. https://doi.org/10.1016/j.intimp.2020.107264.

[58] R. Gao, W. Shu, Y. Shen, et al., Peptide fraction from sturgeon muscle by pepsin hydrolysis exerts anti-inflammatory effects in LPS-stimulated RAW264.7 macrophages via MAPK and NF-κB pathways, Food Sci. Hum. Wellness 10(1) (2021) 103-111. https://doi.org/10.1016/j.fshw.2020.04.014.

[59] O.I. Vitseva, K. Tanriverdi, T.T. Tchkonia, et al., Inducible toll-like receptor and NF-κB regulatory pathway expression in human adipose tissue, Obesity 16(5) (2008) 932-937. https://doi.org/10.1038/oby.2008.25.

[60] J. Hirosumi, G. Tuncman, L. Chang, et al., A central role for JNK in obesity and insulin resistance, Nature 420 (2002) 333-336. https://doi.org/10.1038/nature01137.

[61] Y.T. Kuo, C.C. Lin, H.T. Kuo, et al., Identification of baicalin from Bofutsushosan and Daisaikoto as a potent inducer of glucose uptake and modulator of insulin signaling-associated pathways, J. Food Drug Anal. 27(1) (2019) 240-248. https://doi.org/10.1016/j.jfda.2018.07.002.

[62] R. Zhu, B. Chen, Y. Bai, et al., Lycopene in protection against obesity and diabetes: a mechanistic review, Pharmacol. Res. 159 (2020) 104966. https://doi.org/10.1016/j.phrs.2020.104966.

[63] X. Chen, W. Jiang, Y. Liu, et al., Anti-inflammatory action of geniposide promotes wound healing in diabetic rats, Pharm. Biol. 60(1) (2022) 294-299. https://doi.org/10.1080/13880209.2022.2030760.